Journal of Associated Medical Sciences 2024; 57(2): 132-140

JAMS
Journal of Associated Medical Sciences

Scopus Indexed & Thai-Journal Citation Index Centre (TCI)

Journal of Associated Medical Sciences

Journal homepage: https://www.tci-thaijo.org/index.php/bulletinAMS/index

A comparative study of pre-processing methods to improve glioma segmentation performance in brain MRI using deep learning

Kasatapad Naknaem[1] Titipong Kaewlek[1,2,3*]

[1]Medical Physics Program, Department of Radiological Technology, Faculty of Allied Health Sciences, Naresuan University, Phitsanulok Province, Thailand.
[2]Department of Radiological Technology, Faculty of Allied Health Sciences, Naresuan University, Phitsanulok Province, Thailand.
[3]Interdisciplinary Health and Data Sciences Research Unit, Faculty of Allied Health Sciences, Naresuan University, Phitsanulok Province, Thailand.

ARTICLE INFO

Article history:
Received 17 February 2024
Accepted as revised 17 March 2024
Available online 19 March 2024

Keywords:
Glioma, image segmentation, image enhancement, deep learning, U-net architecture.

ABSTRACT

Background: Glioma is the most common brain tumor in adult patients and requires accurate treatment. The delineation of tumor boundaries must be accurate and precise, which is crucial for treatment planning. Currently, delineating boundaries for tumors is a tedious, time-consuming task and may be prone to human error among oncologists. Therefore, artificial intelligence plays a vital role in reducing these problems.

Objective: This study aims to find a relationship between improving image enhancement and evaluating the performance of deep learning models for segmenting glioma image data on brain MRI images.

Materials and methods: The BraTs2023 dataset was used in this study. The image dataset was converted from three dimensions to two dimensions and then subjected to pre-processing via four image enhancement techniques, including contrast-limited adaptive histogram equalization (CLAHE), gamma correction (GC), non-local mean filter (NLMF), and median and Wiener filter (MWF). Subsequently, it was evaluated for structural similarity index (SSIM) and mean squared error. The deep learning segmentation model was created using the U-Net architecture and assessed for dice similarity coefficient (DSC), accuracy, precision, recall, F1-score, and Jaccard index for tumor segmentation.

Results: The performance of enhanced image results for CLAHE, GC, NLMF, and MWF techniques shows SSIM values of 0.912, 0.905, 0.999, and 0.911, respectively. The dice similarity coefficient (DSC) for segmentation without image enhancement was 0.817. The DSC of segmentation for CLAHE, GC, NLMF, and MWF techniques were 0.818, 0.812, 0.820, and 0.797, respectively.

Conclusion: The enhanced image technique could affect the performance of tumor segmentation. by the enhanced image for use in a trained model may increase or decrease performance depending on the chosen image enhancement technique and the parameters determined by each method.

Introduction

Glioma is the most frequent primary central nervous system cancer in adults, exhibiting extreme intrinsic heterogeneity in appearance, shape, and histology. Gliomas can be classified into high-grade glioma (HGG) and low-grade glioma (LGG). The prognosis of gliomas depends on the grade and genomic profile. HGG is a tumor that shows a severe clinical prognosis and rapid invasion, with a median survival rate of two years or less. It differs from low-grade glioma in that it has a worse prognosis and is more invasive

∗ **Corresponding contributor.**
Author's Address: *Medical Physics Program, Department of Radiological Technology, Faculty of Allied Health Sciences, Naresuan University, Phitsanulok Province, Thailand.*
E-mail address: titipongk@nu.ac.th
doi: 10.12982/JAMS.2024.035
E-ISSN: 2539-6056

or noninvasive.[1,2] Whether HGG or LGG, there is a similarity in the tumor volume, including the whole tumor, tumor core, and active tumor region. As a result, many different types of MR imaging exist because the T1-weighted MRI image can't clearly define the tumor boundary. Therefore, other types of MR imaging, such as T1-contrast, T2-weighted, and T2-FLAIR, are used to indicate the three tumor regions mentioned clearly. Accurate identification of brain tumor sub-regions boundaries in MRI is of profound importance in many clinical applications, such as tumor detection, treatment planning, image-guided procedures, and monitoring tumor growth. However, manual tumor detection and delineation are tedious, time-consuming, and depend on the experience of the oncologist. This may cause human error while delineating the boundaries of the tumor, including disruption of work when dealing with many patients.[3] For the above reasons, automatic tumor boundaries delineation is necessary to reduce the problems mentioned.

The science of deep learning has been used to develop knowledge. Deep learning is a part of the science of artificial intelligence. Since deep learning is more flexible than machine learning, it can automatically find features within image data. For this reason, deep learning is popular in medical image segmentation. Nevertheless, Lin M *et al*. 4's research found a Dice Similarity Coefficient (DSC) of 0.887. The study of Franziska Knuth *et al*.[5] found a DSC of 0.770, and the research of Zhao C *et al*.[6] found a DSC of 0.774. The results depend on various factors, including the architecture used, specific details related to deep learning modeling, and the image quality used to train the deep learning model. The research of Güneş AM *et al*.[7] shows that image quality affects the quality of the segmentation model. When the dataset has increased noise and artifacts during the training of a large dataset, the model's performance increases, which shouldn't be the case. Therefore, the researcher is interested in studying the comparison of pre-processing methods to improve the performance of image segmentation of glioma on brain MRI images using deep learning. The objective is to find a relationship between improving image enhancement and the performance of deep learning models and to develop a deep learning model for segmenting glioma image data on brain MRI images.

Materials and methods

This study conducted a comparative analysis of pre-processing methods aimed at enhancing glioma segmentation performance in brain MRI using deep learning. It consists of two main parts: the first part compares the effectiveness of various pre-processing methods, while the second part assesses the performance of the deep learning model, as shown in Figure 1. Initially, the input image dataset is fed into the program, followed by image pre-processing, which involves converting 3D images to 2D grayscale images and resizing them to 128x128 pixels. Subsequently, the image dataset undergoes enhancement techniques and is evaluated using metrics such as the Structural Similarity Index and the Mean Squared Error. The enhanced dataset is then utilized to train and test the deep learning model. Finally, the model's performance is evaluated using metrics including the Dice similarity coefficient, F1 score, Jaccard similarity coefficient, recall, precision, and accuracy. The result is a predicted mask. The study's detailed aspects include patient data preparation, pre-processing techniques, tumor segmentation architecture, model training, and statistical analysis.

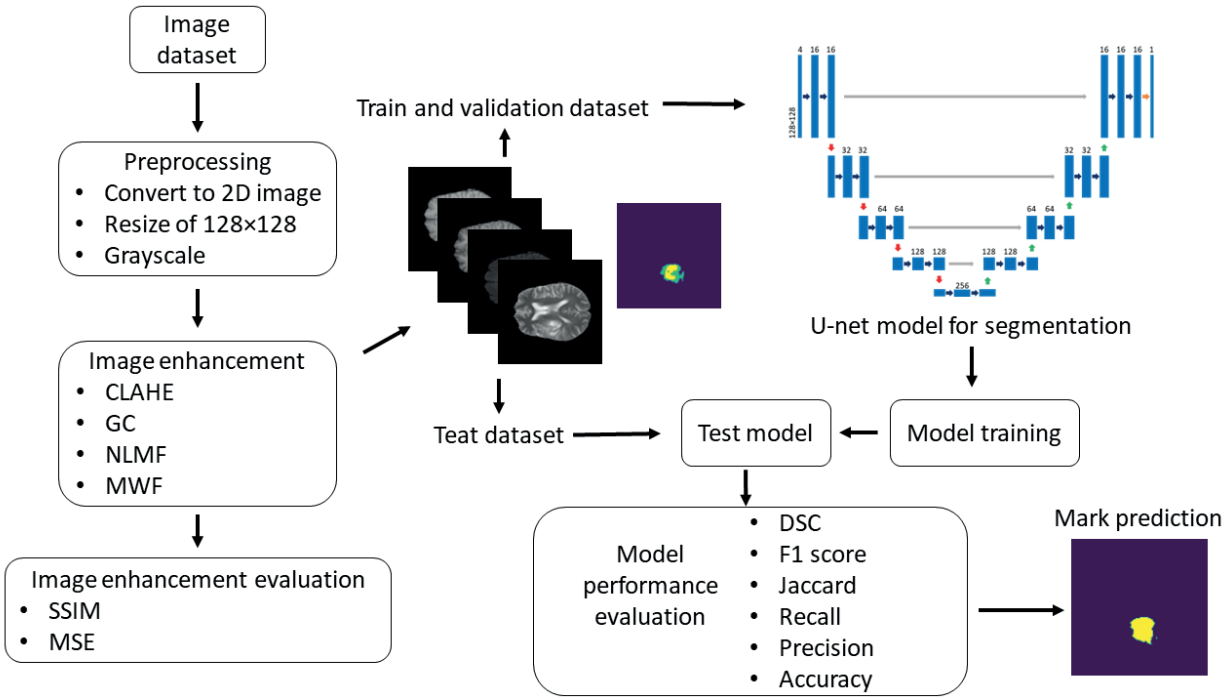

Figure 1 *Workflows of image enhancement and model.*

Patient data preparing

The MR images used in this study were collected from a public dataset, the Brain Tumor Segmentation (BraTS) Challenge 2023 dataset.[1,3,8] The dataset comprises T1, post-contrast T1-weighted (T1Gd), T2-weighted, and T2 Fluid Attenuated Inversion Recovery (T2-FLAIR) MR images of 1,470 brain glioma patients. The volume of 3D MR images is 240×240×155 pixels, and the image voxel size is 1.0 mm^3. The ground truth includes the GD-enhancing tumor region, the peritumoral edematous or invaded tissue region, and the necrotic tumor core region. Experienced neuroradiologists approved these annotations.

Pre-processing technique

The 3D image files in nii.gz format are converted to 2D image files with the png extension. This process involves selecting only the axial MRI images from all four types of MRI images, with the condition that a mask must be present and the extent of the tumor is more than 1% compared to all the data within the mask. The result yields 54,031 axial images for each type. Subsequently, 5,000 images are randomly selected, and the image and mask data are transformed into numpy arrays (npy file extension). Additionally, the images are resized and converted to grayscale, resulting in image and mask data with dimensions of 128×128×1.

This study applies four image enhancement techniques, including contrast-limited adaptive histogram equalization, gamma correction, non-local mean filter, and median and Wiener filter, to enhance the details of all images. Each technique is explained in detail as follows:

Contrast-Limited Adaptive Histogram Equalization (CLAHE)

CLAHE is a technique for reducing noise and over-enhancement by dividing the image into sub-images or tiles. Each tile expands the image intensity range by adjusting the difference in intensity of objects within the image to be similar and limits the height of the histogram by setting a level to eliminate the histogram (clip limit). This distributes the signal exceeding the limit to other parts of the histogram without exceeding the limit.[9,10] This study set the parameters as follows: the clip limit (cl) values and tile sizes (ts) are (0.1, 8×8), (0.2, 2×2), (0.2, 6×6), (0.2, 8×8), and (0.3, 6×6), respectively.

Gamma Correction (GC)

GC is a technique for image processing that adjusts the gamma value according to the characteristics of the image to suit its brightness and contrast.[11,12] Gamma correction is given by the following equation (1). When, the enhanced image will be brighter than the original image, and when, the enhanced image will be darker than the original image. The disadvantage of gamma correction is that it involves an unvaried modification due to a predefined value.[13] This study set the parameters as follows: the gamma values (g) are 0.7, 1.3, 1.5, 1.7, and 1.9, respectively.

$$T(I) = I_{max}\left(\frac{I}{I_{max}}\right)^{\gamma} \quad (1)$$

Where I_{max} is maximum pixel intensity, is pixel intensity, and is gamma correction.

Non-local mean filter

NLMF is an algorithm that filters out noise from images while maintaining the sharpness of the edges of objects within the image. It also adjusts areas within the image to be smoother. NLMF calculates the average of all pixels within the image by considering the similarity between pixels. The resulting averaging eliminates noise and gives the pixels of the image similar values.[14,15] This study set the parameters as follows: set the smoothing kernel value (s), patch size (p), and window size (w) to (1, 6, 20), (1, 7, 15), (1, 7, 20), (2, 2, 20), and (2, 8, 15), respectively.

Median and Wiener filter (MWF)

The Median filter is a filter used to remove noise from images, especially salt and pepper noise. The Median Filter works by taking the pixel values around the position of the pixel of interest, arranging them from least to greatest, and selecting the median value to use. Next, the data is processed through WF to reduce noise and improve signal quality by trying to make the mean square error between the original image and the enhanced image as low as possible.[16] This study set the parameters as follows: set the kernel sizes (k) to 3×3, 5×5, 7×7, 9×9, and 11×11, respectively.

In the final step, all four types (CLAHE, GC, NLMF, and MWF) of MRI images are combined to create a new dataset with a size of 128×128×4. Subsequently, the combined dataset is divided into 4,000 training sets and 1,000 validation sets out of the 5,000 sets of image and mask data. Additionally, 1,000 data sets are randomly selected to create a test set. In each set, the data will include a mask or the boundary of the tumor based on the number of data sets. Therefore, a total of five data sets will be obtained for training the model, comprising a dataset with no image enhancement, a dataset enhanced with the CLAHE technique, a dataset enhanced with the GC technique, a dataset enhanced with the NLMF technique, and a dataset enhanced with the MWF technique.

Tumor segmentation architecture

The U-Net architecture was employed to segment the tumor from the brain tissue area in the brain MRI images. The details of the U-Net for this proposed adaptation were derived from Ronneberger *et al*.,[17] and the structure consists of an encoder path, decoder path, and connecting path. These three paths follow the typical architecture of a conventional network. The encoder path comprises two 3×3 convolutions, with each layer followed by a rectified linear unit (ReLU) and a 2×2 max-pooling operation with two strides for downsampling. With each downsampling step, the number of feature channels increases twofold. On the other hand, the decoder path consists of two 3×3

convolutions, with each layer followed by ReLU and 2×2 up-convolutions for upsampling. With each upsampling step, the number of feature channels decreases twofold. The decoder path is concatenated with the encoder path through the connecting path, linking to the corresponding feature map from the encoder path. Finally, the last layer consists of a 1×1 convolution, utilizing a sigmoid activation function for the final output, as shown in Figure 2.

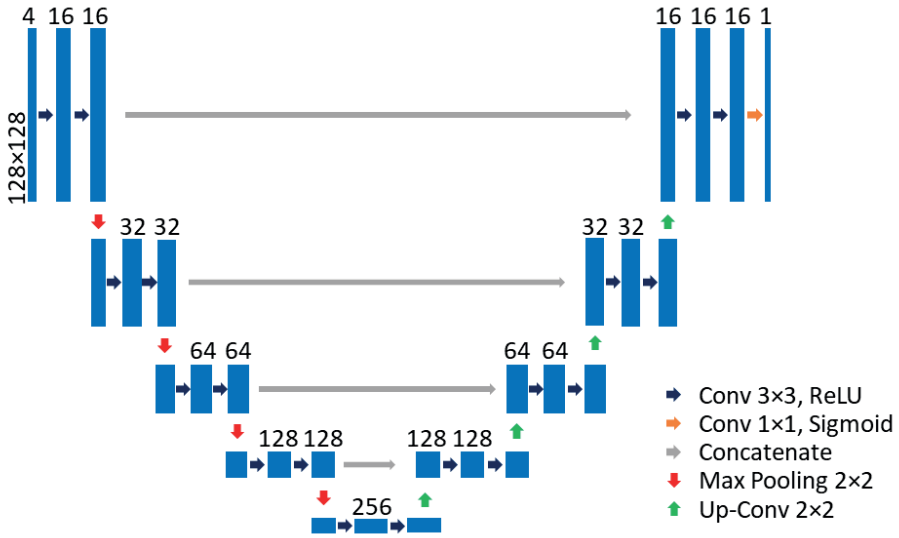

Figure 2 *U-Net architecture of this study.*

Model training

The training used Tensorflow version 2.13 as the backend in Python version 3.10.9, utilizing an NVIDIA GeForce RTX 3050 Laptop GPU. The image segmentation model was trained to employ the Adam optimizer, a learning rate set at 0.001 with a lower bound on the learning rate of 0.0000001, a Dice Similarity Coefficient (DSC) loss function, and a batch size of 32 for 100 epochs. Initially, the model underwent training with a combination image dataset without image enhancement. Throughout the training process, the model was validated using a validation dataset to estimate errors in the training. The early stopping technique was employed to mitigate the overfitting problem. Upon completing the training of the model with the combination image dataset without image enhancement, the dataset was modified to a combination image dataset with image enhancement using four techniques (CLAHE, GC, NLMF, and MWF).

Statistical analysis

The statistical analysis is divided into image enhancement and segmentation model performance.

For image enhancement, evaluation involves using the structural similarity index (SSIM) and mean squared error (MSE). SSIM serves as a metric (luminance, contrast, and structure) to measure the similarity between two given images. At the same time, MSE is employed to compare the true pixel values of the original image to the degraded image. The equations for SSIM and MSE are provided in (2)-(3).

$$SSIM = i(x,y) \times c(x,y) \times s(x,y) \quad (2)$$

Where i is the luminance similarity index, c is the contrast similarity index, s is the structure similarity index, x is the original image, and y is the enhanced image.

$$SSIM = \frac{1}{mn} \sum_0^{m-1} \sum_0^{n-1} | |f(i,j)-g(i,j)| |^2 \quad (3)$$

Where f is the original pixel image, g is the enhanced pixel image, m is the row number of image, n is the column number of image, i is the row index, and j is the column index.

The model performance is assessed through the confusion matrix, which consists of values such as the dice similarity coefficient (DSC), Jaccard similarity coefficient, accuracy, precision, sensitivity (recall), and F1-score. The evaluation values for model performance are presented in equations (4)-(9).

$$DSC = \frac{2|A \cap B|}{|A| + |B|} \quad (4)$$

$$Jaccard = \frac{|A \cap B|}{|A| + |B| - |A \cap B|} \quad (5)$$

Where A and B are datasets A and B, and $A \cap B$ is the intersection part of the two datasets.

$$Accuracy = \frac{TP + TN}{TP+TN+FP+FN} \quad (6)$$

$$Precision = \frac{TP}{TP + FP} \quad (7)$$

$$Recall = \frac{TP}{TP + FN} \quad (8)$$

$$F1\ score = \frac{2 \times precision \times recall}{precision \times recall} \quad (9)$$

Where True Positives (TP) is the model predicting a tumor boundary when it is a tumor boundary, True Negatives (TN) is the model correctly predicting it not to be a tumor boundary, False Positive (FP) is the model predicting a tumor boundary when it is not a tumor boundary, and False Negative (FN) is the model predicting something different than the tumor boundary.

Results

Evaluation of image enhancement

Table 1 shows the results of the evaluation parameters for each image enhancement. NLMF exhibits the highest SSIM compared to other techniques, followed by GC, MWF, and CLAHE, respectively. Regarding the MSE value, NLMF has the lowest MSE compared to other techniques, followed by CLAHE, GC, and MWF, respectively.

Table 1 Results of the image enhancement techniques.

Technique	Parameter	T1		T1c		T2		T2f	
		SSIM	MSE	SSIM	MSE	SSIM	MSE	SSIM	MSE
CLAHE No.1	cl= 0.1, ts=8	0.721	395.03	0.695	288.53	0.701	314.16	0.703	460.31
CLAHE No.2	cl=0.2, t=2	0.914	6.013	0.91	11.64	0.912	7.358	0.912	8.381
CLAHE No.3	cl=0.2, ts=6	0.743	108.31	0.721	156.38	0.732	92.08	0.735	113.68
CLAHE No.4	cl=0.2, ts=8	0.721	395.03	0.695	288.53	0.701	314.16	0.703	460.31
CLAHE No.5	cl=0.3, ts=6	0.743	108.31	0.721	156.38	0.732	92.08	0.735	113.68
GC No.1	g=0.7	0.923	1231.2	0.895	2388.57	0.896	2260.82	0.905	1834.04
GC No.2	g=1.3	0.956	684.21	0.938	1311.27	0.94	1241.86	0.945	1012.54
GC No.3	g=1.5	0.959	624.8	0.938	1167.96	0.94	1107.54	0.947	912.38
GC No.4	g=1.8	0.957	601.61	0.929	1045.05	0.933	995.04	0.943	845.03
GC No.5	g=1.9	0.956	607.09	0.924	1020.6	0.929	973.67	0.94	838.26
NLMF No.1	s=1, p=6, w=20	0.999	0.007	0.999	0.015	0.999	0.006	0.999	0.001
NLMF No.2	s=1, p=7, w=15	0.999	0.006	0.999	0.014	0.999	0.001	0.999	0.006
NLMF No.3	s=1, p=7, w=20	0.999	0.007	0.999	0.015	0.999	0.006	0.999	0.001
NLMF No.4	s=2, p=2, w=20	0.999	0.015	0.998	0.212	0.999	0.169	0.999	0.116
NLMF No.5	s=2, p=8, w=15	0.999	0.061	0.999	0.114	0.999	0.023	0.999	0.059
MWF No.1	k = 3	0.957	1080.54	0.836	4242.03	0.912	1376.93	0.939	1021.88
MWF No.2	k = 5	0.95	1105.33	0.834	4340.87	0.906	1474.32	0.929	1057.57
MWF No.3	k = 7	0.942	1132.57	0.832	4425.22	0.897	1572.39	0.919	1092.08
MWF No.4	k = 9	0.932	1160.39	0.829	4497.25	0.888	1668.26	0.908	1125.35
MWF No.5	k = 11	0.922	1188.02	0.825	4560.84	0.878	1760.5	0.898	1157.18

Evaluation of model performance for segmentation

Figure 3 shows the learning curves of the model during training with a dataset, with and without the image enhancement process. We can observe that all models don't exhibit a gap between training and validation loss; as a result, none of the models suffer from overfitting or underfitting problems.

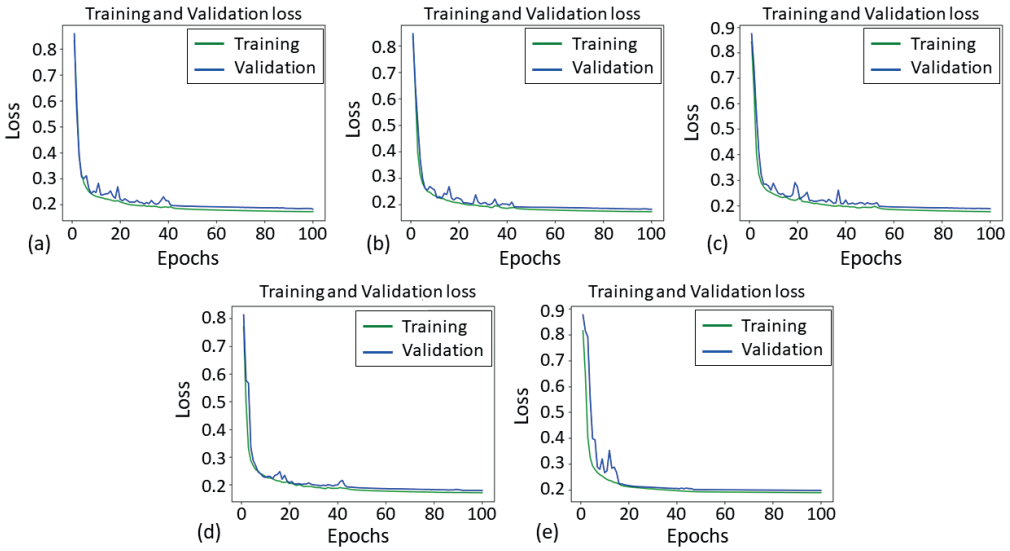

Figure 3 *Loss curve of training and validation set. a: standard MRI image dataset without image enhancement, b-e: MRI image dataset with image enhancement (CLAHE, GC, NLMF, and MWF, respectively).*

Table 2 presents the results of the evaluation parameters for various models. A trained model with original MRI images has a DSC of 0.8171 compared to a trained model with MRI images via image enhancement techniques. We can observe that CLAHE and NLMF techniques can increase the DSC value, while GC and MWF techniques decrease the DSC value. Specifically, CLAHE, NLMF, GC, and MWF have a maximum DSC of 0.818, 0.820, 0.812, and 0.797, respectively, in this study.

Table 2 The performance of tumor segmentation in various models.

Technique	Parameter	DSC	F1	Jaccard	Recall	Precision	Accuracy
Normal	-	0.817	0.892	0.815	0.943	0.860	0.994
CLAHE No.1	cl=0.1, ts=8	0.817	0.896	0.820	0.943	0.865	0.994
CLAHE No.2	cl=0.2, ts=2	0.818	0.895	0.818	0.940	0.866	0.994
CLAHE No.3	cl=0.2, ts=6	0.811	0.884	0.801	0.926	0.858	0.994
CLAHE No.4	cl=0.2, ts=8	0.814	0.888	0.806	0.938	0.854	0.994
CLAHE No.5	cl=0.3, ts=6	0.812	0.886	0.805	0.931	0.858	0.994
GC No.1	g=0.7	0.812	0.885	0.801	0.922	0.861	0.994
GC No.2	g=1.3	0.811	0.890	0.809	0.930	0.863	0.994
GC No.3	g=1.5	0.808	0.878	0.792	0.923	0.851	0.993
GC No.4	g=1.8	0.803	0.872	0.782	0.917	0.844	0.993
GC No.5	g=1.9	0.802	0.870	0.780	0.917	0.843	0.993
NLMF No.1	s= 1, p=6, w=20	0.819	0.899	0.824	0.942	0.870	0.994
NLMF No.2	s=1, p=7, w=15	0.819	0.895	0.818	0.950	0.856	0.994
NLMF No.3	s=1, p=7, w=20	0.820	0.900	0.826	0.946	0.869	0.994
NLMF No.4	s=2, p=2, w=20	0.819	0.898	0.823	0.940	0.870	0.994
NLMF No.5	s=2, =8, w=15	0.820	0.900	0.827	0.948	0.867	0.994
MWF No.1	k=3	0.797	0.866	0.774	0.900	0.851	0.993
MWF No.2	k=5	0.792	0.859	0.763	0.893	0.842	0.992
MWF No.3	k=7	0.781	0.846	0.744	0.880	0.831	0.992
MWF No.4	k=9	0.789	0.855	0.755	0.892	0.833	0.992
MWF No.5	k=11	0.761	0.816	0.702	0.854	0.800	0.990

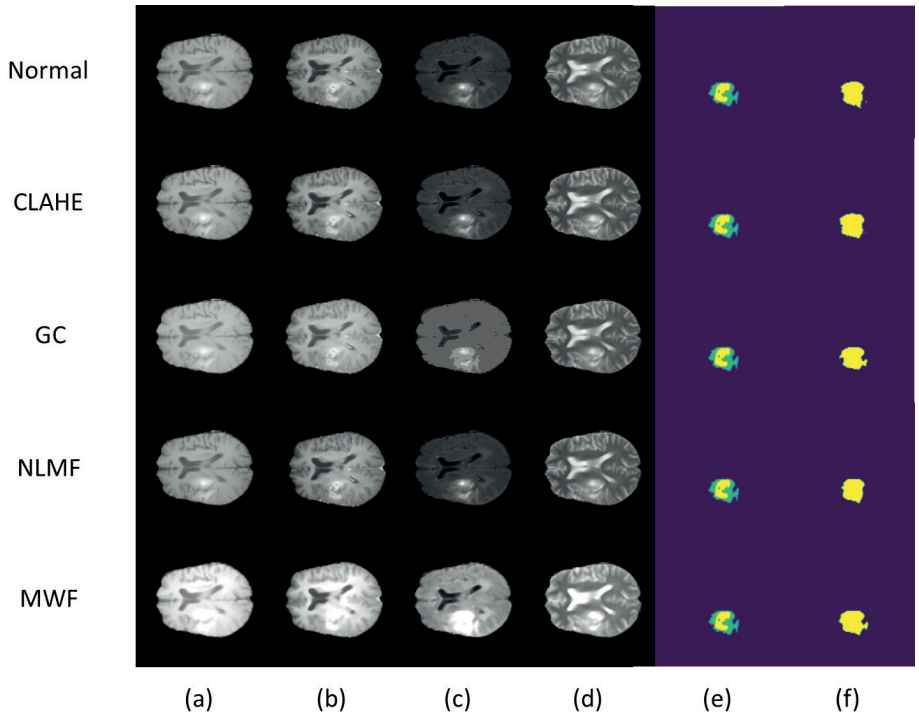

Figure 4 *Image of image enhancement and mark prediction from the model. A: T1-weighted, b: post-contrast T1, c: T2-weighted, d: T2-FLAIR, e: gound truth or mask, e: mask prediction.*

Table 3 compares each image enhancement technique's DSC and average SSIM values.

Table 3 Comparative of DSC and average SSIM values.

Technique	Parameter	DSC	Average SSIM
CLAHE No.1	cl=0.1, ts=8	0.817	0.705
CLAHE No.2	cl=0.2, ts=2	0.818	0.912
CLAHE No.3	cl=0.2, ts=6	0.811	0.733
GC No.1	g=0.7	0.812	0.905
GC No.2	g=1.3	0.811	0.945
GC No.3	g=1.5	0.808	0.946
NLMF No.1	s=1, p=6, w=20	0.819	0.999
NLMF No.2	s=1, p=7, w=15	0.819	0.999
NLMF No.5	s=2, p=8, w=15	0.820	0.999
MWF No.1	k=3	0.797	0.911
MWF No.4	k=9	0.789	0.889
MWF No.5	k=11	0.761	0.881

Discussion

This study examines the relationship between image enhancement and the performance of deep learning models, comparing the results of enhancement techniques to increase the efficiency of glioma tumor segmentation on brain MRI images. Four image quality enhancement techniques, CLAHE, GC, NLMF, and MWF, are used to assess image quality based on SSIM and MSE values. Additionally, this report investigates a deep learning model for glioma tumor image segmentation on brain MRI images, developing the model using the U-net architecture. The study compares models trained with image datasets that have undergone all four image enhancement techniques.

Regarding the relationship between image enhancement and deep learning model performance, it was observed that image quality significantly impacts the performance of deep learning models, as indicated in Table 3 when comparing the same techniques. For instance, the trained model with the CLAHE technique (CLAHE No. 1), featuring a cliplimit parameter of 0.1 and a tile size of 8, displayed a DSC value of 0.817 and an SSIM value of 0.705. In comparison, adjusting the parameters to cliplimit equal to 0.2 and tile size equal to 6 (CLAHE No. 3) resulted in a DSC value of 0.811 and an SSIM value of 0.733. It is evident that, despite the improved image quality of the CLAHE No. 3 model, it reduces the efficiency of the model. Furthermore, models trained with datasets of similar image quality exhibited varying performance, as seen in the CLAHE No.2 and MWF No.1 models, in the MWF No.4 and MWF No.5 models, and the GC No.2 and GC No.3 models. These results indicate that poorer image quality may contribute to better model performance, aligning with the research by Güneş AM *et al.*, which stated that reducing the image quality of training data by reducing contrast or adding artifacts makes the resulting model more effective.[7]

The developed deep learning model for glioma tumor segmentation on brain MRI images revealed that trained models with datasets that did not undergo image enhancement techniques had a DSC value of 0.817, while the image segmentation trained model with the CLAHE enhancement technique had a DSC value of 0.818, GC had a DSC value of 0.812, NLMF had a DSC value of 0.820, and MWF had a DSC value of 0.797. Table 3 indicates that the model with image enhancement using the NLMF technique has the highest DSC value, while the model with image enhancement using the MWF technique has the least, being 2.4% lower than the trained model without image enhancement techniques. Table 2 shows that the F1-score, Jaccard, recall, precision, and accuracy values of the trained model without image enhancement techniques were 89.2%, 81.5%, 94.3%, 86.0%, and 99.4%, respectively. For the trained models with the CLAHE technique, the values were 89.5%, 81.8%, 94.0%, 86.6%, and 99.4%, respectively. The GC values were 88.5%, 80.1%, 92.2%, 86.1%, and 99.4%, respectively. NLMF values were 90.0%, 82.7%, 94.8%, 86.7%, and 99.4%, respectively, and MWF values were 86.6%, 77.4%, 90.0%, 85.1%, and 99.3%, respectively.

Comparing the trained model with the enhanced dataset with previous works on glioma segmentation on brain MRI images, Table 4 shows that the DSC values of the U-Net+CLAHE, U-Net+GC, U-Net+NLMF, and U-Net+CLAHE models are lower than all previous works, both in the trained model with similar and completely different datasets. Adding image enhancmore than ement techniques alone is sufficient to increase model performance. However, the proposed model accuracy and recall demonstrate high performance for all models, at least 0.993 for U-Net+MWF, close to Ghosh S. 2019[18] and Al Nasim MA 2022.[19]

Table 4 Compares of previous works.

Author	Image	Network	Recall	Precision	Accuracy	DSC
Ghosh S. 2019[18]	TCGA-LGG	U-Net+ResNeXt50	-	-	0.996	0.932
		U-Net+FPN	-	-	0.993	0.899
Al Nasim MA 2022[19]	BraTS2019	U-Net+empirical analysis	0.997	-	0.998	0.920
Manasa K. 2022[20]	Brast2018	U-Net+Zernile Moments	0.877	0.810	-	0.852
Yan C. 2022[21]	BraTS2018	SEResU-Net	0.923	-	-	0.911
Our proposed	BraTS2023	U-Net+CLAHE	0.940	0.866	0.994	0.818
		U-Net+GC	0.922	0.861	0.994	0.812
		U-Net+NLMF	0.948	0.867	0.994	0.820
		U-Net+MWF	0.900	0.851	0.993	0.797

Limitation

Limitations related to this study: First, using image datasets in two dimensions may reduce the quality of model training because the original image dataset used for training is designed in 3D. Second, different types of MRI images should be separated for enhancement because each type has distinct characteristics. However, this study used the same parameters for enhanced images in each technique since the mask design is used to label the tumor's boundaries, designed for all four MRI types together. Finally, this study did not introduce imperfections within the dataset to compare image enhancements, which would help better understand the relationship between increased image enhancement and model performance.

Conclusion

In conclusion, the study explores the relationship between image enhancement and the performance of deep learning models, aiming to develop a deep learning model for segmenting glioma tumors on MRI images using the U-net architecture with image enhancement techniques. The results demonstrate that pre-processing significantly improves image quality and can enhance brain segmentation on brain MRI images. Specifically, the non-local mean filter technique performed best, followed by gamma correction, median and wiener filter technique, and contrast-limited adaptive histogram equalization was the lowest. However, when using enhanced images for trained models, it was found that image enhancement techniques can increase performance, precisely the non-local mean filter technique, the contrast-limited adaptive histogram equalization technique, while the gamma correction technique and the median and wiener filter decrease model performance. Enhanced images for trained models may increase or decrease performance depending on the chosen image enhancement technique and the parameters determined by each method.

Conflict of interest

None

Funding

None

Ethical approval

The study was approved by the ethics committee of Naresuan University, Thailand (IRB No. P1-0155/2566).

References

[1] Baid U, Ghodasara S, Mohan S, Bilello M, Calabrese E, Colak E, *et al*. The rsna-asnr-miccai brats 2021 benchmark on brain tumor segmentation and radiogenomic classification. arXiv. 2021; 2107.02314. doi.org/10.48550/arXiv.2107.02314

[2] Lin M, Momin S, Lei Y, Wang H, Curran WJ, Liu T, *et al*. Fully automated brain tumor segmentation from multiparametric MRI using 3D context deep supervised U-Net. Med Phys. 2021; 48(8): 4365-74. doi.org/10.1002/mp.15032.

[3] Menze BH, Jakab A, Bauer S, Kalpathy-Cramer J, Farahani K, Kirby J, *et al*. The multimodal brain tumor image segmentation benchmark (BRATS). IEEE Trans Med Imaging. 2014; 34(10): 1993-2024. doi: 10.1109/TMI.2014.2377694.

[4] Lin M, Momin S, Lei Y, Wang H, Curran WJ, Liu T, *et al*. Fully automated brain tumor segmentation from multiparametric MRI using 3D context deep supervised U-Net. Med Phys. 2021; 48(8): 4365-74. doi.org/10.1002/mp.15032.

[5] Knuth F, Adde IA, Huynh BN, Groendahl AR, Winter RM, Negård A, *et al*. MRI-based automatic segmentation of rectal cancer using 2D U-Net on two independent cohorts. Acta Oncol. 2022; 61(2): 255-63. doi.org/10.1080/0284186X.2021.2013530.

[6] Zhao C, Zhao Z, Zeng Q, Feng Y. MVP U-Net: Multi-view pointwise U-Net for brain tumor segmentation. InBrainlesion: Glioma, Multiple Sclerosis, Stroke and Traumatic Brain Injuries: BrainLes 2020, Lecture Notes in Computer Science, October 4, 2020: Lima, Peru, 12659: 93-103. Springer, Cham. doi.org/10.1007/978-3-030-72087-2_9

[7] Güneş AM, van Rooij W, Gulshad S, Slotman B, Dahele M, Verbakel W. Impact of imperfection in medical imaging data on deep learning-based segmentation performance: An experimental study using synthesized data. Med Phys. 2023; 50(10): 6421-32. doi: 10.1002/mp.16437

[8] Bakas S, Akbari H, Sotiras A, Bilello M, Rozycki M, Kirby JS, *et al*. Advancing the cancer genome atlas glioma MRI collections with expert segmentation labels and radiomic features. Sci Data. 2017; 4(1): 1-3. doi.org/10.1038/sdata.2017.117.

[9] Wen H, Qi W, Shuang L. Medical X-ray image enhancement based on wavelet domain homomorphic filtering and CLAHE. Proceedings of In 2016 International Conference on Robots & Intelligent System (ICRIS), IEEE. 2016 Aug 27: 249-54. doi: 10.1109/ICRIS.2016.50.

[10] Zuiderveld K. Contrast limited adaptive histogram equalization. Graphics gems. 1994; 474-85. doi.org/10.1016/B978-0-12-336156-1.50061-6.

[11] Cao G, Huang L, Tian H, Huang X, Wang Y, Zhi R. Contrast enhancement of brightness-distorted images by improved adaptive gamma correction. Comput Electr Eng. 2018; 66: 569-82. doi.org/10.1016/j.compeleceng.2017.09.012.

[12] Huang Z, Zhang T, Li Q, Fang H. Adaptive gamma correction based on cumulative histogram for enhancing near-infrared images. Infrared Phys Technol. 2016; 79: 205-15. doi.org/10.1016/j.infrared.2016.11.001.

[13] Sahnoun M, Kallel F, Dammak M, Mhiri C, Mahfoudh KB, Hamida AB. A comparative study of MRI contrast enhancement techniques based on Traditional Gamma Correction and Adaptive Gamma Correction: Case of multiple sclerosis pathology. Proceedings of In 2018 4th international conference on advanced technologies for signal and image processing (ATSIP), IEEE. 2018 Mar 21, 1-7. doi: 10.1109/ATSIP.2018.8364467.

[14] Shreyamsha Kumar BK. Image denoising based on non-local means filter and its method noise thresholding. SIViP. 2013; 7: 1211-27. doi.org/10.1007/s11760-012-0389-y

[15] Chandrashekar L, Sreedevi A. Assessment of non-linear filters for MRI images. Proceedings of In 2017 2nd International Conference on Electrical, Computer and Communication Technologies (ICECCT), IEEE. 2017 Feb 22, 1-5. doi: 10.1109/ICECCT.2017.8117852.

[16] Min A, Kyu ZM. MRI images enhancement and tumor segmentation for brain. In2017 18th International Conference on Parallel and Distributed Computing, Applications and Technologies (PDCAT) 2017 Dec 18 (pp. 270-275). IEEE. doi: 10.1109/PDCAT.2017.00051.

[17] Ronneberger O, Fischer P, Brox T. U-net: Convolutional networks for biomedical image segmentation. Proceedings of InMedical Image Computing and Computer-Assisted Intervention-MICCAI 2015: 18th International Conference, Munich, Germany, October 5-9, 2015, 234-241). Springer, Cham. doi.org/10.1007/978-3-319-24574-4_28.

[18] Ghosh S, Santosh KC. Tumor segmentation in brain MRI: U-Nets versus feature pyramid network. Proceedings of In2021 IEEE 34th International Symposium on Computer-Based Medical Systems (CBMS), IEEE. 2021 Jun 7, 31-6. doi: 10.1109/CBMS52027.2021.00013.

[19] Al Nasim MA, Al Munem A, Islam M, Palash MA, Haque MM, Shah FM. Brain tumor segmentation using enhanced u-net model with empirical analysis. In2022 25th International Conference on Computer and Information Technology (ICCIT) 2022 Dec 17 (pp. 1027-32). IEEE. doi: 10.1109/ICCIT57492.2022.10054934.

[20] Manasa K, Krishnaveni V. Brain Tumor Segmentation Using Zernike Moments in U-Net. In 2022 International Conference on Intelligent Innovations in Engineering and Technology (ICIIET) 2022 Sep 22 (pp. 342-6). IEEE. doi: 10.1109/ICIIET55458.2022.9967618.

[21] Yan C, Ding J, Zhang H, Tong K, Hua B, Shi S. SEResU-Net for Multimodal Brain Tumor Segmentation. IEEE Access. 2022; 10: 117033-44. doi: 10.1109/ACCESS.2022.3214309.